

# Known-Interference Cancellation Over Time-Varying Rayleigh-Fading Channels

Karel Pärlin\*, Aaron Byman†, Tommi Meriläinen†, and Taneli Riihonen\*

\*Tampere University, Finland

†Bittium, Finland

e-mail: karel.parlin@tuni.fi

**Abstract**—Security and covertness are both essential properties of wireless tactical communications that can be introduced at the physical layer of these systems through cooperative jamming. The concept relies on sharing in advance the jamming waveform or means to generate it with cooperative receivers, and using that knowledge to cancel out the jammer’s impact through known-interference cancellation (KIC) while non-cooperative receivers cannot do the same. A promising KIC method is the frequency offsets-compensated least mean squares (FO-LMS) algorithm that iteratively updates its estimates of the wireless channel as well as carrier and sampling frequency offsets proportionally to user-defined step sizes. The iterative updates inevitably cause misadjustments, the extent of which the step sizes affect. In time-varying conditions, selecting the step sizes becomes a trade-off between the algorithm’s tracking performance and the extent of misadjustments. In this work, we characterize that trade-off and the optimal step size over Rayleigh-fading channels with Jakes’ Doppler spectrum through theoretical expressions. Supporting simulation and measurement results are provided, which demonstrate the accuracy and advantage of the optimal step size expression compared to exhaustive search methods.

## I. INTRODUCTION

Cooperative jamming can provide physical layer security and covertness to wireless tactical communications between authorized nodes while also limiting that between unauthorized nodes if the jamming signal can be canceled or avoided by the former but not by the latter [1], [2]. It has been demonstrated that by having the cooperative jammer transmit an interference signal that is in advance known to the authorized receiver nodes (e.g., by the generating algorithm and a seed), these benefits can be achieved by using known-interference cancellation (KIC) methods at authorized receiver nodes to suppress the effects of jamming [3]–[5] as illustrated in Fig. 1.

The KIC method in [4], [5] is based on the frequency offsets-compensated least mean squares (FO-LMS) algorithm that, by having knowledge of the original transmitted signal, estimates and tracks the wireless channel as well as carrier and frequency offsets between a transmitter and receiver [6]. The method has also been extended to handle multiple received known interference (KI) signals simultaneously [7], a bandlimited received KI of a wideband transmitted KI [8], and

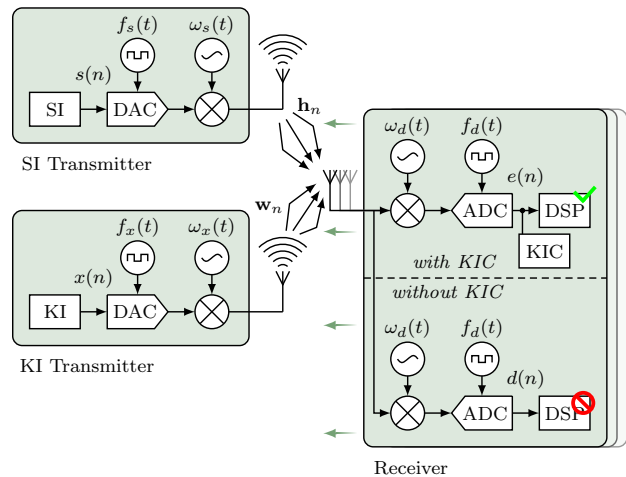


Fig. 1. Known interference (KI) can prevent unauthorized electromagnetic spectrum access as long as the authorized nodes can cancel the KI, which in practice is often complicated by a rapidly time-varying environment.

nonlinear distortions in the received KI [5], therefore solving several of the issues that could arise in practical systems.

The FO-LMS and its extensions [4]–[8] rely on the stochastic gradient descent principle, iteratively updating estimates of the modeled parameters proportionally to user-defined step sizes. In stationary environments, the choice of gradient descent step sizes generally presents a tradeoff between speed of adaptation and misadjustment [9]. In time-varying environments, the choice of step sizes further presents a tradeoff between tracking capability and misadjustment [10]. Tracking performance of classical adaptive filters has been extensively studied considering autoregressive channel models [10], [11].

The performance of the FO-LMS algorithm has been studied comprehensively in stationary environments [6]. However, results for estimating the FO-LMS’s performance in time-varying environments or for selecting the step sizes that are optimal under such conditions are missing in the literature. Thus, in this paper, we study the FO-LMS’s performance in terms of its mean squared error (MSE) when tracking a Rayleigh-fading channel with Jakes’ Doppler spectrum and analyze the effect that time-varying environments have on KIC. An expression for selecting the channel estimation step size for optimal tracking performance is also provided, which offers a significant advantage over brute-force searching.

This research work was supported by the Finnish Research Impact Foundation, the Research Council of Finland, and the Finnish Support Foundation for National Defence.

### A. System Model

The challenges of KIC in time-varying environments follow from the system model in Fig. 1. The signal of interest (SI) transmitter sends a signal  $s(n)$  that is unknown but of interest to the receiver. The KI transmitter sends a signal  $x(n)$  that is either known or unknown but of no interest to the receiver. The superposed discrete-time signal with variance  $\sigma_d^2$  at the receiver becomes

$$d(n) = \mathbf{w}_n^H \mathbf{y}_n e^{j\hat{\phi}(n)} + \mathbf{h}_n^H \mathbf{s}_n + v(n), \quad (1)$$

where  $\mathbf{w}_n$  and  $\mathbf{h}_n$  are the time-varying channel impulse responses from the KI and SI transmitters to the receiver, respectively,  $\{\cdot\}^H$  denotes conjugate transpose,  $v(n)$  is measurement noise with variance  $\sigma_v^2$ ,  $\mathbf{y}_n$  denotes  $x(n)$  resampled with a time-varying frequency offset  $\eta(n)$  according to (2) in [6], and the multiplicative term  $e^{j\hat{\phi}(n)} = e^{j\sum_{i=1}^n \epsilon(i)}$  accounts for the carrier frequency offset and phase noise.

Not knowing  $x(n)$ , an unauthorized receiver is left with the superposition of the received signals. Knowing  $x(n)$ , however, an authorized receiver can subtract it from the received signal by

$$e(n) = d(n) - \hat{\mathbf{w}}_n^H \hat{\mathbf{y}}_n e^{j\hat{\phi}(n)} \stackrel{\text{ideally}}{=} \mathbf{h}_n^H \mathbf{s}_n + v(n), \quad (2)$$

if it can provide  $\hat{\mathbf{w}}_n$ ,  $\hat{\epsilon}(n)$ , and  $\hat{\eta}(n)$  as accurate estimates of  $\mathbf{w}_n$ ,  $\eta(n)$ , and  $\epsilon(n)$ , respectively. With good parameter estimates, the KI is canceled and the error in (2) contains mainly the SI and unavoidable measurement noise.

The FO-LMS algorithm [6, Algorithm 1] updates its parameter estimates by minimizing the error in (2) so that

$$\hat{\mathbf{w}}_n = \hat{\mathbf{w}}_{n-1} + \mu_w \hat{\mathbf{y}}_n e^{j\hat{\phi}(n)} e^*(n), \quad (3a)$$

$$\hat{\epsilon}(n) = \hat{\epsilon}(n-1) + \mu_\epsilon \Im \left\{ \hat{\mathbf{w}}_{n-1}^H \hat{\mathbf{y}}_n e^{j\hat{\phi}(n)} e^*(n) \right\}, \quad (3b)$$

$$\hat{\eta}(n) = \hat{\eta}(n-1) + \mu_\eta \Re \left\{ \hat{\mathbf{w}}_{n-1}^H \hat{\mathbf{y}}_n' e^{j\hat{\phi}(n)} e^*(n) \right\}, \quad (3c)$$

where  $\hat{\mathbf{y}}_n'$  is the derivative of  $\hat{\mathbf{y}}_n$ , and  $\mu_w$ ,  $\mu_\epsilon$ , and  $\mu_\eta$  are the channel, carrier, and sampling frequency offset estimation step sizes, respectively. The challenge is to choose them properly.

## II. TRACKING PERFORMANCE

In order to make the following analysis more tractable, we rely on few reasonable assumptions. Firstly, we assume that the KI and SI are both white Gaussian signals ( $\mathbf{R} = \sigma_x^2 \mathbf{I}$  and  $\mathbf{S} = \sigma_s^2 \mathbf{I}$ ), which implies statistical independence between the signals themselves, between the signals and the measurement noise, as well as the signals and the time-varying channels. Furthermore, we herein assume that the frequency offsets change slowly so that small step sizes  $\mu_\epsilon$  and  $\mu_\eta$  can be used, leading to negligible impact from the update equations (3b) and (3c) on the algorithm's steady-state misadjustment. Finally, and without loss of generality, we normalize the gains of the channels  $\mathbf{w}_n$  and  $\mathbf{h}_n$  to unity.

Then, the minimum MSE that the FO-LMS algorithm can reach with perfect adaptation is  $J_{\min} = \sigma_d^2 - \sigma_x^2 = \sigma_v^2 + \sigma_s^2$ .

However, due to the misadjustment of the algorithm, the MSE in steady state becomes

$$J(\infty) = \lim_{n \rightarrow \infty} J(n) = J_{\min} + J_{\text{ex}}(\infty), \quad (4)$$

where  $J_{\text{ex}}(\infty)$  is the steady-state excess mean squared error (EMSE) as  $n$  approaches infinity. In order to estimate the effect that FO-LMS has on the SI processing when using it to cancel the KI from the total received signal (1), it is necessary to be able to calculate that EMSE.

It has been previously shown that for time-varying channels that correspond to a first-order autoregressive model without the impact of carrier and sampling frequencies, the EMSE of the classical least mean squares (LMS) adaptive filter becomes [11], [12]

$$J_{\text{ex}}(\infty) = \frac{\mu_w M \sigma_x^2 J_{\min} + \frac{M \sigma_q^2}{\mu_w}}{2 - \mu_w (M + 1) \sigma_x^2}, \quad (5)$$

where  $M$  is the number of filter coefficients used to model the channel impulse response and  $\sigma_q^2$  is the variance of the first-order autoregressive model according to channel fading.

The second term of the EMSE increases with  $\sigma_q^2$  and decreases with  $\mu_w$  leading to the optimal step size

$$\mu_w^{\text{opt}} = \sqrt{\frac{\sigma_q^2}{J_{\min} \sigma_x^2}}. \quad (6)$$

Unfortunately, that model does not usually match practical situations. The widely accepted model to represent time-varying fading in wireless communications is the Rayleigh-fading channel model with Jakes' Doppler spectrum [13], [14]. It has been previously observed that good analytical approximations of the Jakes' model's time-variance can be attained with first- and second-order autoregressive models [15]–[17], for which the variance of the random channel perturbations can be expressed as  $\sigma_q^2 = \sqrt{1 - J_0^2(2\pi f_D T)}$ , where  $J_0(\cdot)$  is the zeroth-order Bessel function of the first kind,  $f_D$  is the Doppler frequency, and  $T$  is the sampling period [18].

Still, the precision of (5) can be considerably improved. The update in (3a) can be derived as a steady-state version of a Kalman filter based on a random walk model [19], [20] and considering then the update process in (3a) as a first-order time-invariant filter in the complex frequency domain [21], [22], the misadjustment and tracking error of the iterative updates can be more accurately approximated as

$$J_{\text{ex}}(\infty) \approx \frac{\mu_w M \sigma_x^2 J_{\min} + \frac{M \sigma_q^2}{\mu_w} \cdot \frac{1}{\mu_w M \sigma_x^2}}{2 - \mu_w (M + 1) \sigma_x^2}. \quad (7)$$

Here, the EMSE again increases with  $\sigma_q^2$ , but decreases with  $\sigma_x^2$  and more importantly decreases quadratically with  $\mu_w$ , which is significant in accurately predicting the EMSE. The optimal step size can be found by taking the derivative of (7) with respect to  $\mu_w$  and finding its roots, leading to

$$\mu_w^{\text{opt}} \approx \frac{3\sigma_q^2}{J_{\min} \sigma_x^2 \sqrt[3]{\frac{\sqrt{\frac{3^6 2^4 \sigma_q^4}{J_{\min}^2} + \frac{3^6 2^2 \sigma_q^6}{M^2 \sigma_x^8}}}{2} - \frac{3^3 2 \sigma_q^2}{J_{\min} M \sigma_x^4}}}. \quad (8)$$

### III. SIMULATIONS

In order to verify the theoretical findings, we compared the theoretical results to simulation results.

#### A. Simulation Setup

The simulations were carried out according to the system model described in Section I-A and illustrated in Fig. 1. The KI and noise floor were simulated as white Gaussian noise with unit variance  $\sigma_x^2 = 1$  and  $\sigma_v^2 = 0.00032$ , respectively, resulting in an interference-to-noise ratio (INR) of 35 dB. The SI was simulated as a 128-subcarrier OFDM signal, which can be considered roughly Gaussian under the central limit theorem [23]. The OFDM subcarriers were modulated using QPSK and the total signal had a variance specified by the signal-to-interference-plus-noise ratio (SINR) as given in the forthcoming figures. The signals were simulated with sampling frequency  $f_x = 10$  MHz and carrier frequency  $f_c = 875$  MHz. The sampling and carrier frequency offsets between the KI transmitter and receiver were 1 Hz and 100 Hz, respectively.

The channel between the KI transmitter and receiver was simulated using the TU-6 non-line-of-sight (NLOS) channel model with Rayleigh-fading taps [24]. The TU-6 channel model has a delay spread of  $5\mu\text{s}$ , requiring in this case  $M \geq 51$  taps to model. The FO-LMS was run with  $M = 70$  taps to mimic practical scenarios where the the channel is unknown and the FO-LMS algorithm benefits from the extra taps in aligning the expected and received KI signals. The carrier and sampling frequency offset update step sizes were set to  $\mu_\epsilon = 10^{-11}$  and  $\mu_\eta = 10^{-11}$ . Without reducing the challenge of KIC, the channel between the SI transmitter and receiver was simplified to a line-of-sight (LOS) static and frequency-flat channel model. This expedited the SI processing, which is not the main focus of this work but an additional measure for assessing the KIC performance.

#### B. Simulation Results

Figs. 2 and 3 show the FO-LMS's simulated and estimated EMSE depending on the channel update step size  $\mu_w$  at different SINRs and receiver velocities. The figures also show the optimal step sizes  $\mu_w^{\text{opt}}$  estimated based on (8) for each of the studied SINR and velocity combination. The simulated and theoretical results are in close agreement in the close-to-optimal step size range and the estimated optimal step sizes result in the lowest possible EMSE. Furthermore, the impact of both the SI and receiver mobility is clearly evident. As the SINR or the receiver velocity increases, the EMSE inevitably increases too, even with an optimal channel update step size.

Fig. 4 shows the simulated pre-KIC and post-KIC SI demodulation symbol error rates (SERs) depending on the channel update step size  $\mu_w$  at different INRs as well as the estimated optimal step sizes  $\mu_w^{\text{opt}}$  for each of the studied INRs. These results demonstrate that KIC directly improves the SI processing, and that the EMSE-wise optimal channel update step size  $\mu_w^{\text{opt}}$  provides excellent results also in terms of the post-KIC SER.

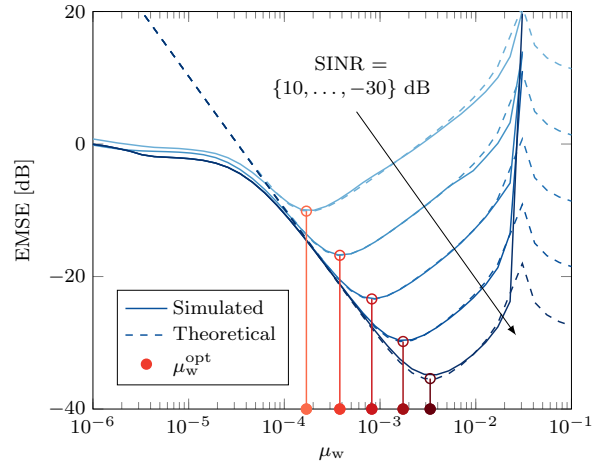


Fig. 2. EMSE of the FO-LMS algorithm with a receiver velocity of 25.0 m/s depending on the channel update step size  $\mu_w$  and SINR. Optimal step sizes at different SINRs calculated based on (8) are shown on the x-axis.

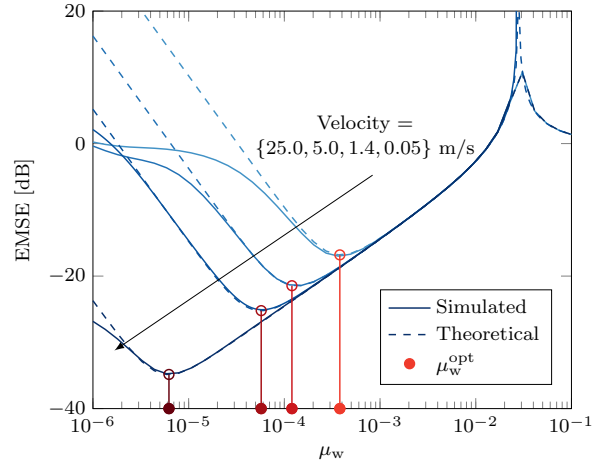


Fig. 3. EMSE of the FO-LMS algorithm with a SINR of 0 dB depending on the channel update step size  $\mu_w$  and receiver velocity. Optimal step sizes at different velocities calculated based on (8) are shown on the x-axis.

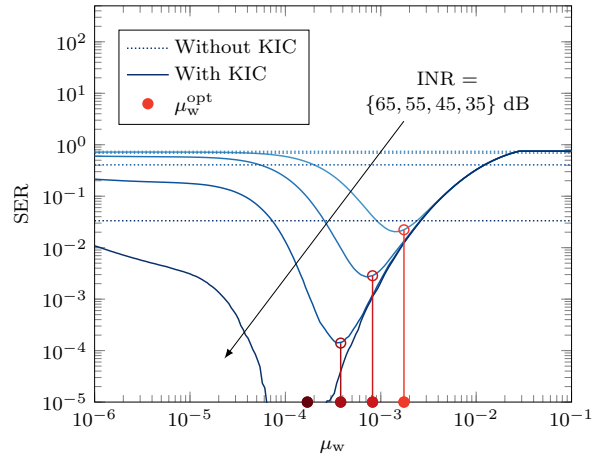


Fig. 4. SI demodulation SER with a SNR of 10 dB, receiver velocity of 25.0 m/s, and depending on the step size  $\mu_w$  and INR. Optimal step sizes at different INRs calculated based on (8) are shown on the x-axis.

#### IV. MEASUREMENTS

We also compared the theoretical results to measurements-based results to verify practical applicability.

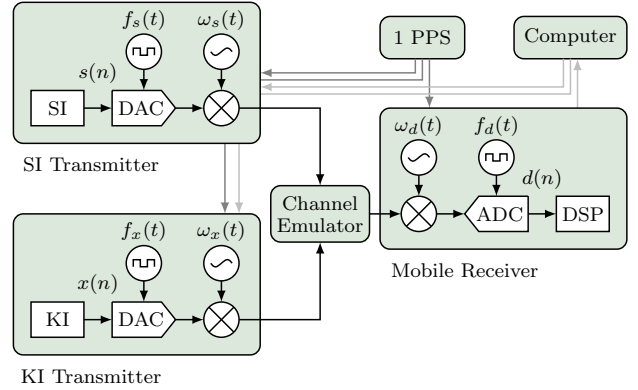
##### A. Measurement Setup

We carried out the measurements using the setup illustrated in Fig. 5. Specifically, we used three USRP-2900 software-defined radios (SDRs) as the nodes in the system model and connected the two transmitting SDRs to the receiving one via a Keysight PROPSIM FS16 channel emulator. Equivalently to the simulations in the previous section, the channel emulator in the measurements emulated the TU-6 channel for the KI path, whereas the SI was passed through a static frequency-flat channel. In order to simplify working with the measurements, the radios were connected to a 1 PPS synchronizer, which allowed to start the nodes at the same time but has no impact on the channel or the carrier and sampling frequency offsets. Furthermore, a digital intermediate frequency was used to prevent the IQ imbalances and LO leakages [25] from affecting the measurement results. With these settings, we carried out a comprehensive measurement campaign by varying the received KI power in a 65 dB range and the received SI power in a 35 dB range, both with 2 dB steps, covering a wide range of relevant SINRs. We recorded the measurements to the computer and processed them offline.

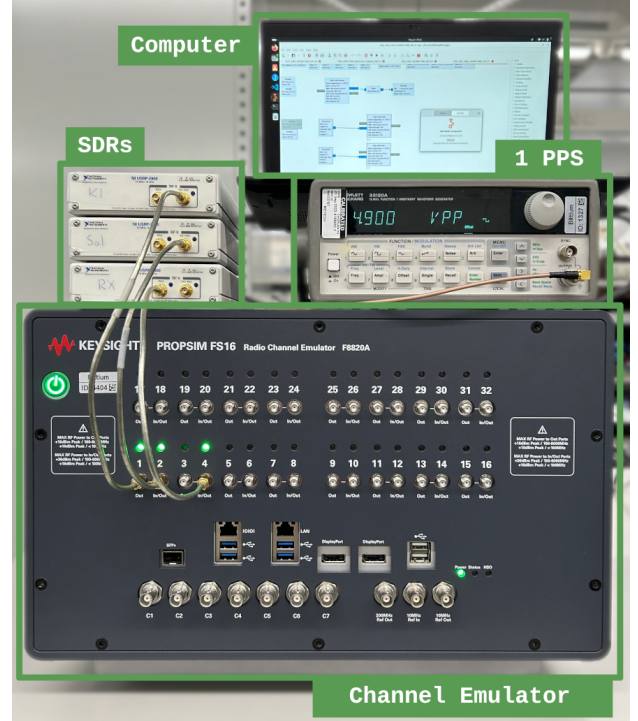
##### B. Measurement Results

Since the EMSE is difficult to extract from measurement results, we herein refer to the MSE instead. Fig. 6 and 7 compare the FO-LMS's measured and theoretical MSEs at different INRs and velocities without SI. These results show a good match between the measured and theoretical MSE values at lower INRs and across the studied receiver velocities but the results start to disagree as the received INR increases. This is likely because the theoretical analysis does not account for the fluctuations in the radios' carrier and sampling frequencies, including phase noise and sampling jitter, that additionally limit the KIC performance at high INRs in practice. Despite the mismatch in MSE at higher INRs, the estimated optimal step size  $\mu_w^{\text{opt}}$  still achieves close-to-minimal MSE. As in the simulated cases in Fig. 2 and 3, the measurements results here again highlight the impact that the receiver velocity has on the KIC feasibility. As the channel becomes more time varying, the range of step sizes that minimize the MSE becomes smaller and having a well-chosen channel update step size becomes more critical.

Results including the SI are illustrated in Fig. 8. Specifically, Fig. 8 shows the measured pre-KIC and post-KIC SI demodulation SERs depending on the channel update step size  $\mu_w$  at different SINRs as well as the estimated optimal step sizes  $\mu_w^{\text{opt}}$  for each of the studied SINRs. The results in Fig. 8, as in in the simulated case illustrated in Fig. 4, again show that canceling the KI leads to improvements in the SI processing proportionally to the KIC and that the step size  $\mu_w^{\text{opt}}$  that minimizes the MSE also minimizes the SER.



(a) Diagram of the measurement setup



(b) Photo of the measurement setup

Fig. 5. Measurement setup with three USRP-2900 SDRs and a Keysight PROPSIM FS16 channel emulator.

Finally, Fig. 9 shows the SERs achieved over the entire measurement grid without and with KIC, using  $\mu_w$  based on either exhaustive search that minimizes the SER or calculated based on (8). The results show that the calculated optimal step size  $\mu_w^{\text{opt}}$  results in SERs very close to these produced with exhaustively searched optimal step sizes  $\mu_w$ . This is an important result as it allows KIC to be run without the computational overhead that otherwise comes from the need to exhaustively search for the optimal channel update step size. The results also show the extent by which KIC can improve or facilitate the SI processing under cooperative jamming. At lower receiver velocities the SI processing is improved by up to 35 dB whereas at higher receiver velocities that improvement is reduced to some extent.

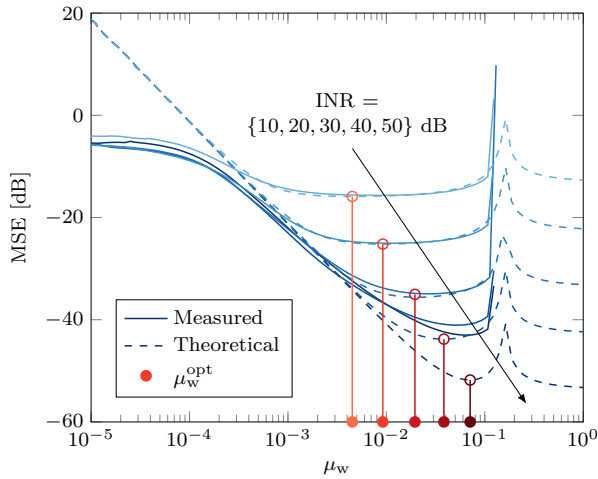


Fig. 6. MSE and the optimal step size  $\mu_w^{\text{opt}}$  of the FO-LMS algorithm at different INRs with the velocity fixed at 25.0 m/s and without the SI.

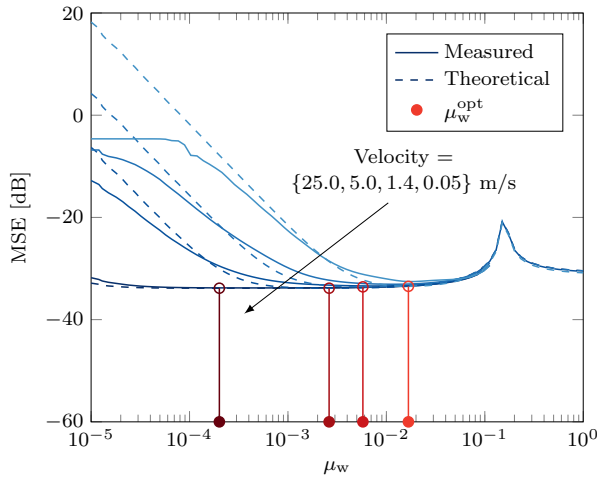


Fig. 7. MSE and the optimal step size  $\mu_w^{\text{opt}}$  of the FO-LMS algorithm at different velocities with the INR fixed at 28 dB and without the SI.

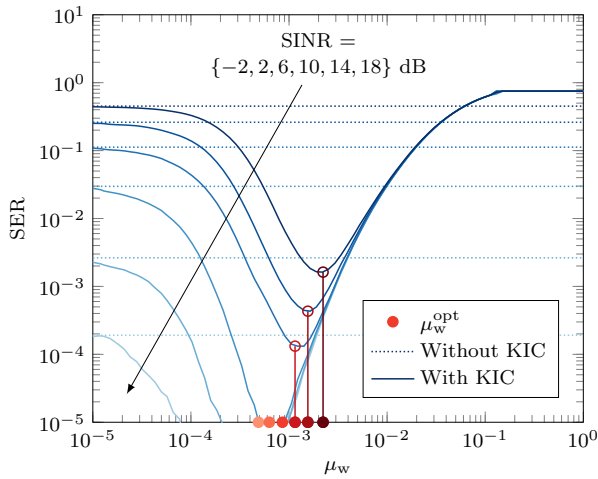


Fig. 8. SI demodulation SER at different SINRs with receiver velocity of 25.0 m/s and INR of 25 dB. Optimal step sizes at different SINRs calculated based on (8) are shown on the x-axis.

## V. CONCLUSION

This work addresses the challenge of reliable known-interference cancellation (KIC) in time-varying wireless channels. Specifically, the feasibility of KIC under time-varying Rayleigh-fading channels with Jakes' Doppler spectrum is analyzed using the frequency offsets-compensated least mean squares (FO-LMS) algorithm. In time-varying environments, the algorithm's performance and the selection of its step sizes becomes a trade-off between tracking ability and steady-state estimation misadjustment. This work provides closed-form expressions for estimating the algorithm's excess mean squared error (EMSE) and for calculating the optimal channel estimation step size depending on the channel characteristic. By providing the closed-form expression for the optimal step size, this work fills an important gap in physical layer KIC design, offering scalable and low-overhead tuning for real-time systems. Supporting simulation and measurement results are provided, which demonstrate the accuracy of the expressions.

## REFERENCES

- [1] J. M. Hamamreh, H. M. Furqan, and H. Arslan, "Classifications and applications of physical layer security techniques for confidentiality: A comprehensive survey," *IEEE Communications Surveys & Tutorials*, vol. 21, no. 2, pp. 1773–1828, Oct. 2018.
- [2] C. Gao, B. Yang, D. Zheng, X. Jiang, and T. Taleb, "Cooperative jamming and relay selection for covert communications in wireless relay systems," *IEEE Transactions on Communications*, vol. 72, no. 2, pp. 1020–1032, Feb. 2024.
- [3] W. Guo, H. Zhao, and Y. Tang, "Testbed for cooperative jamming cancellation in physical layer security," *IEEE Wireless Communications Letters*, vol. 9, no. 2, pp. 240–243, Feb. 2020.
- [4] K. Pärilin, T. Riihonen, M. Turunen, V. Le Nir, and M. Adrat, "Known-interference cancellation in cooperative jamming: Experimental evaluation and benchmark algorithm performance," *IEEE Wireless Communications Letters*, vol. 12, no. 9, pp. 1598–1602, Sep. 2023.
- [5] K. Pärilin, M. Turunen, A. Byman, T. Meriläinen, V. Le Nir, M. Adrat, and T. Riihonen, "High-power cooperative jamming with nonlinear known-interference cancellation," *IEEE Transactions on Aerospace and Electronic Systems*, vol. 61, no. 3, pp. 7193–7204, Jun. 2025.
- [6] K. Pärilin, T. Riihonen, V. Le Nir, and M. Adrat, "Estimating and tracking wireless channels under carrier and sampling frequency offsets," *IEEE Transactions on Signal Processing*, vol. 71, pp. 1053–1066, Mar. 2023.
- [7] K. Pärilin, T. Riihonen, M. Turunen, V. Le Nir, and M. Adrat, "Distributed cooperative jamming with multi-reference known-interference cancellation," in *Proc. International Conference on Military Communications and Information Systems*, Apr. 2024.
- [8] K. Pärilin, V. Le Nir, T. Meriläinen, A. Byman, M. Adrat, and T. Riihonen, "Wideband cooperative jamming with band-limited known-interference cancellation," in *Proc. IEEE Military Communications Conference*, Oct. 2024.
- [9] R. H. Kwong and E. W. Johnston, "A variable step size LMS algorithm," *IEEE Transactions on Signal Processing*, vol. 40, no. 7, pp. 1633–1642, Jul. 1992.
- [10] E. Eweda, "Comparison of RLS, LMS, and sign algorithms for tracking randomly time-varying channels," *IEEE Transactions on Signal Processing*, vol. 42, no. 11, pp. 2937–2944, Nov. 1994.
- [11] N. R. Yousef and A. H. Sayed, "Ability of adaptive filters to track carrier offsets and channel nonstationarities," *IEEE Transactions on Signal Processing*, vol. 50, no. 7, pp. 1533–1544, Jul. 2002.
- [12] —, "A unified approach to the steady-state and tracking analyses of adaptive filters," *IEEE Transactions on Signal Processing*, vol. 49, no. 2, pp. 314–324, Feb. 2001.
- [13] R. H. Clarke, "A statistical theory of mobile-radio reception," *Bell system technical journal*, vol. 47, no. 6, pp. 957–1000, Jul. 1968.

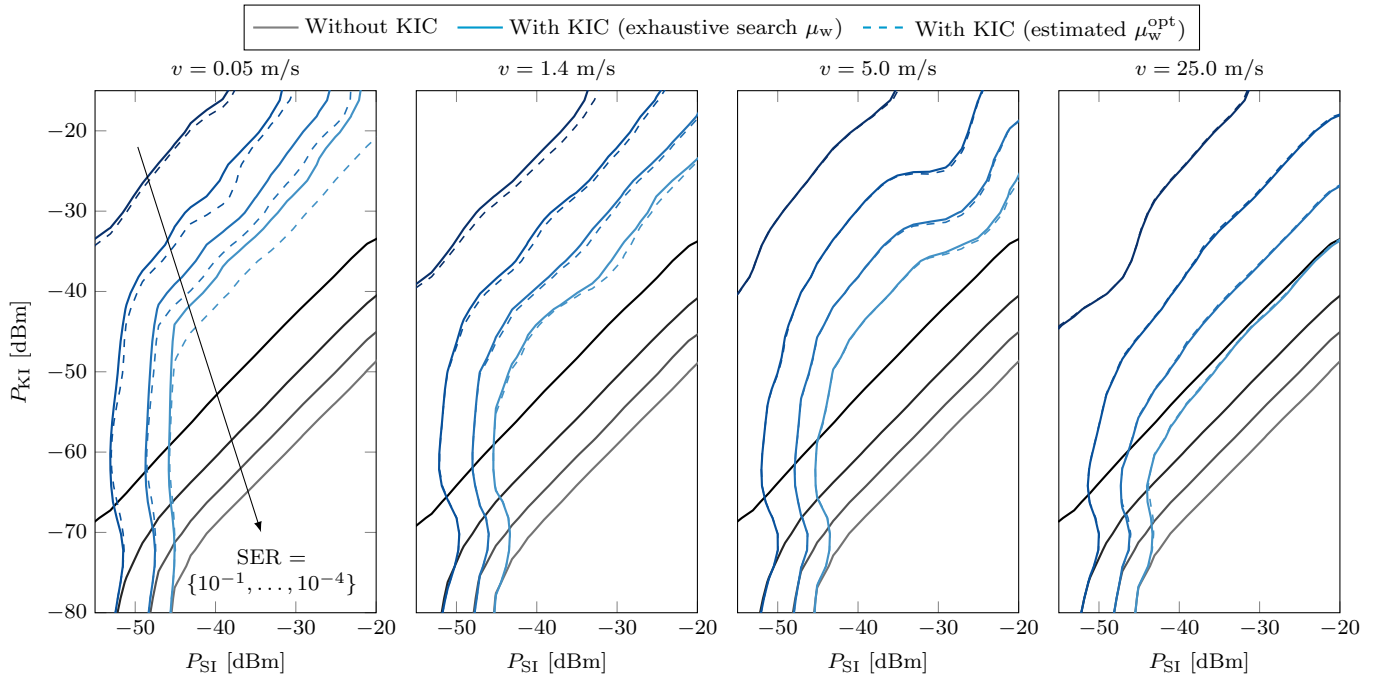


Fig. 9. Measurements-based KIC performance in terms of its impact on the SI processing. KIC is carried out using optimal channel estimation step size based on either exhaustive search ( $\mu_w$ ) or theoretical estimation ( $\mu_w^{\text{opt}}$ ).

- [14] W. C. Jakes and D. C. Cox, *Microwave mobile communications*. Wiley-IEEE press, Sep. 1994.
- [15] J. Galdino and E. Pinto, "A simulation study of adaptive filtering applied to MLSE-PSP receivers," in *Proc. IEEE Military Communications Conference*, Oct. 1998, pp. 338–342.
- [16] J. F. Galdino, E. L. Pinto, and M. S. de Alencar, "Analytical performance of the LMS algorithm on the estimation of wide sense stationary channels," *IEEE Transactions on Communications*, vol. 52, no. 6, pp. 982–991, Jun. 2004.
- [17] A. H. El Husseini, E. P. Simon, and L. Ros, "Second-order autoregressive model-based Kalman filter for the estimation of a slow fading channel described by the Clarke model: Optimal tuning and interpretation," *Digital Signal Processing*, vol. 90, pp. 125–141, Jul. 2019.
- [18] K. E. Baddour and N. C. Beaulieu, "Autoregressive modeling for fading channel simulation," *IEEE Transactions on Wireless Communications*, vol. 4, no. 4, pp. 1650–1662, Jul. 2005.
- [19] L. Lindbom, M. Sternad, and A. Ahlén, "Tracking of time-varying mobile radio channels — Part I: The Wiener LMS algorithm," *IEEE Transactions on Communications*, vol. 49, no. 12, pp. 2207–2217, Dec. 2001.
- [20] L. Lindbom, A. Ahlén, M. Sternad, and M. Falkenström, "Tracking of time-varying mobile radio channels — Part II: A case study," *IEEE Transactions on Communications*, vol. 50, no. 1, pp. 156–167, Jan. 2002.
- [21] R. Gerzaguët, L. Ros, J.-M. Brossier, S. Ghandour-Haidar, and F. Belvèze, "Self-adaptive stochastic Rayleigh flat fading channel estimation," in *Proc. 18th International Conference on Digital Signal Processing*, Jul. 2013.
- [22] L. Sekokotoana, F. Takawira, and O. Oyerinde, "Successive interference cancellation-inspired channel estimation for downlink non-orthogonal multiple access," *Transactions on Emerging Telecommunications Technologies*, vol. 32, no. 10, May 2021.
- [23] S. Wei, D. L. Goeckel, and P. A. Kelly, "Convergence of the complex envelope of bandlimited OFDM signals," *IEEE Transactions on Information Theory*, vol. 56, no. 10, pp. 4893–4904, Oct. 2010.
- [24] ETSI, "TS 100 910 v8.20.0 (2005-11)," *Digital cellular telecommunications system (Phase 2+)—Radio Transmission and Reception—3GPP TS 05.05 version 8.20*, 2005.
- [25] W. Guo, M. Jin, H. Zhao, and S. Shao, "Cooperative jamming cancellation with time-frequency mismatch, IQ imbalance and LO leakage for secure communications," *IEEE Transactions on Wireless Communications*, 2025, early access.